Carbon 144 (2019) 269–279

Contents lists available at ScienceDirect

Carbon

journal homepage: www.elsevier.com/locate/carbon

Expanding graphene properties by a simple S-doping methodology based on cold CS_2 plasma

V.K. Abdelkader-Fernández [a], M. Domingo-García [b], F.J. López-Garzón [b], Diana M. Fernandes [a], Cristina Freire [a], Mª Dolores López de la Torre [c], M. Melguizo [c], Mª Luz Godino-Salido [c], Manuel Pérez-Mendoza [b, *]

[a] REQUIMTE/LAQV, DQB, F. de Ciéncias, Universidade do Porto, 4169-007, Porto, Portugal
[b] Dpt. de Q. Inorgánica, Facultad de Ciencias, Universidad de Granada, 18071, Granada, Spain
[c] Dpt. de Química Inorgánica y Orgánica, Universidad de Jaén, 23071, Jaén, Spain

ARTICLE INFO

Article history:
Received 26 October 2018
Received in revised form
5 December 2018
Accepted 14 December 2018
Available online 14 December 2018

ABSTRACT

For the first time, graphene has been successfully doped with sulfur via short exposition to CS_2 microwave cold plasmas, avoiding high-temperature and time/chemicals-consuming treatments. Different S-doped samples were obtained by varying the duration of plasma treatments, reaching a remarkable 2.3 at % of S content after only 5 min of exposition. The S-doped graphenes present several sulfur containing moieties, among which thioether groups resulted to be predominant. These moieties are covalently bond to graphene layers and exhibit good thermal and water stability. In addition, unlike others more conventional methods, S-doping via CS_2 plasmas do not damage the structural order of graphene. The influence of sulfur doping on the graphene properties has been assessed through two different tests: on one side, the capture of Pd^{2+} ions in aqueous solution, and on the other, the electrocatalytic activity towards the production of oxygen from water (OER process). In both cases, the performance of the pristine graphene was significantly enhanced with S-doping. In addition, the capture of Pd^{2+} allows the formation of sulfur-Pd nanoclusters supported on the graphene surface, which are very useful in electrochemical devices.

1. Introduction

The fascinating properties of carbon nanomaterials (graphene, carbon nanotubes (CNTs), etc.) attract enormous interest regarding their potential applications in electronics, electrocatalysis, energy storage and sensors (among others) fields. In addition, the physicochemical characteristics of nanocarbons can be altered via functionalization, improving some of their intrinsic characteristics and hence opening new possibilities for the functionalized derivatives [1]. For example, it has been reported that doped graphene shows better behavior as electrocatalyst than its pristine counterpart [2]. Very high reactive species are needed for an effective functionalization because of the chemical inertness of graphene. The functionalization can result in the modification of the sp^2 C structure, although it can remain almost unaltered when the attachment is produced in terminal carbon atoms (edges) and/or defects. The electronic properties can be conveniently tuned depending on the electronegativity and the size of the guest atom if a substitutional doping is produced. Thus, the band gap energy level, the n- or p-type semiconductive character and the work-function can be tailored by a proper doping/functionalization of graphene [3,4]. Moreover the surface energy, mechanical properties and chemical reactivity are also changed so that the range of application is expanded.

At first boron, nitrogen, oxygen and fluorine [5–8] were the heteroatoms more frequently used for carbon materials doping due to their atomic sizes are not very different to carbon. Then atoms of the third and fourth row of the periodic table, i.e. Cl, Si, S, P and Br, were attached [2,9,10]. Among these atoms sulfur is used for doping carbon materials with different purposes as to modify the physical and chemical characteristics of porous/activated carbons [11–16]. Moreover graphene has been also doped with sulfur for its use in several electrochemical applications [15,17–19]. Thus, sulfur-doped graphene is attracting growing interest as low amounts of sulfur

* Corresponding author.
E-mail address: mjperezm@ugr.es (M. Pérez-Mendoza).

https://doi.org/10.1016/j.carbon.2018.12.045
0008-6223/

can be enough to obtain materials with better electrocatalytic behavior than metal based electrodes. Procedures for doping with sulfur, including post-synthesis and during synthesis, have been reported. The former usually involves the treatment at high temperature of a carbon material with a sulfur-containing precursor. This has been carried out for decades since pioneering works [20,21] which reported doping active carbons by annealing with CS_2 as sulfur source [4,12]. The "during synthesis" procedures consist in the high temperature carbonization of the carbon and sulfur precursors. There are also solvothermal/hydrothermal methods in solution involving some precursors. All these time-consuming processes require harsh conditions, several reactants and high temperatures.

A different approach is to generate highly reactive sulfur radical species which are able to chemically attack the low reactive graphene sheets. This can be achieved by the generation of cold plasma from an S-containing precursor. We have reported the functionalization of some carbon materials, including multi-wall carbon nanotubes and graphene nanoplatelets, with chemical functions by using cold plasma of different precursors [5–8,10]. Moreover the modification of several 2D materials by several plasmas has also been reported [22]. Thus, the aim of this paper is to dope graphene with sulfur by using microwave cold plasma of CS_2. The plasma of this precursor results in several species, among which $S^{\bullet}$ and S^{+} are very reactive towards the graphene sheet. The advantage of this procedure is that it requires short treatments (minutes) and avoids harsh conditions and chemicals (only CS_2). Furthermore the temperature of reaction is very close to room temperature so that no damage of graphene sp^2 structures due to high temperatures is expected.

Moreover we have assessed the impact of plasma S-doping on (i) the capacity of graphene to capture Pd(II) from aqueous solution and on (ii) its electrocatalytic performance towards oxygen evolution reaction (OER). The former pursues the possibility of obtaining S/Pd nanoparticles supported on graphene. This possibility is based on the capture of Pd^{2+} by the sulfur-doped graphene due to the character of Pearson's soft base of sulfur. It is known supported palladium/S compounds are of great interest in several hydrogenation processes as for example the selective alkyne hydrogenation [23]. Moreover graphene-supported sulfur-transition metal nanoparticles are useful in electrochemical energy storage devices [24]. This is due to two factors: on the one hand to the transition metal-sulfur nanoparticles have specific capacities larger than their oxide counterpart thus increasing the performance [25]; on the other to the synergistic properties of graphene/sulfur-transition metal nanoparticles increase the electrochemical performance of energy storage devices [26]. Thus it is considered that graphene is the ideal support to obtain graphene-supported sulfur-transition metal nanoparticles for electrode materials [27,28]. Nevertheless, the preparation of graphene-supported sulfur-transition metal nanoparticles usually involves the sulfidation of supported metallic palladium with SH_2. Therefore, we are proposing a much easier option to obtain these Pd/S nanoparticles supported on graphene. Regarding the OER tests, the evaluation of the S-doping effect on the graphene catalytic activity is directly motivated by the fact that the effective application of graphene-based materials to the energy sector [2,29–32] will be directly conditioned by their electrocatalytic behavior. The scarce studies in which this single-doped material is tested for the OER, always employ harsh-condition-synthetized S-doped graphenes [17,33–36].

2. Experimental

A commercial graphene sample (#2191 YJ) from NanoAmor (USA) has been used. According to the manufacturer the product has a carbon content >98 wt%, a size between 2 and 10 μm and consists of 1–3 layers. The functionalization with sulfur has been carried out by using a plasma generator device (Junior PLC Advanced SP) from Europlasma (Belgium). A scheme of the experimental setup is shown in Fig. 1.

The equipment basically consists of a reaction chamber (ii in Fig. 1) equipped with a microwave source of 2,45 GHz (i in Fig. 1) to generate plasma of several precursors, including gases or liquids. The chamber is connected to several gas and vapor inlets (iv and v) to introduce the precursors, and the flows are controlled by mass-flow controllers (vi). In a typical experiment, around 0.1 g of graphene were put in the reaction chamber. Then the vacuum pump (vii) is connected to the chamber in order to partially remove the air to a residual pressure of around 20–50 mTorr. Helium then is flowed through the chamber for 5 min while pumping down the system in order to remove the residual air. This procedure is repeated three times and in the last one when the vacuum (20–50 mTorr) is reached, CS_2 is flowed (6 cm^3 min^{-1}) into the chamber by connecting the liquid canister (iii in Fig. 1) to the reaction chamber. A dynamic CS_2 vapor pressure of ≈130 mTorr was set and then the plasma of CS_2 was generated by switching on the microwave source (700 w), adjusting the treatment time between 0.5 and 5 min. The samples obtained by these treatments are labelled G-CS_2-t, where t stands for the time of plasma treatment in minutes. In order to study the stability of the sulfur containing groups in solution, the sample G-CS_2-5 was kept stirring in distilled water at room temperature for 24 h. After that the sample was relabeled as G-CS_2-5-w. The analysis of the samples has been carried out by X-ray Photoelectron Spectroscopy (XPS), thermal programmed desorption (TPD), Raman spectroscopy and nitrogen adsorption.

The XPS spectra were obtained in a Kratos Axis Ultra-DLD spectrometer. Monochromatic AlK_{α} radiation in the constant analyzer energy mode with pass energies of 160 and 20 eV for the survey and high resolution spectra, respectively, was used. The survey spectra allowed obtaining the chemical surface composition (at %) of the samples. The deconvolutions of the high resolution spectra allowed analyzing the chemical environments of the surface atoms. This has been carried out by using CASA XPS software.

The thermal stability of the heteroatoms covalently attached to the graphene surface was studied by TPD. For this purpose, the

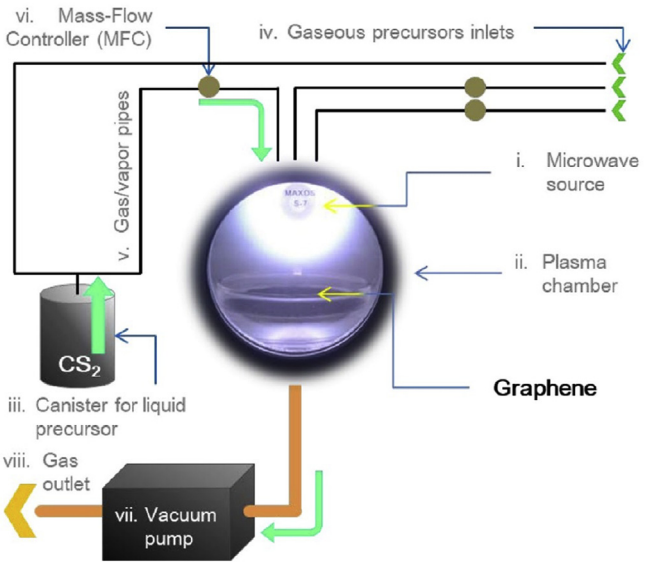

Fig. 1. Scheme of the microwave plasma setup. (A colour version of this figure can be viewed online.)

samples were previously heat-treated in helium flow (50 mL min^{-1}) at 120 °C for two hours and then the temperature was ramped at 10 °C·min^{-1} up to 900 °C. The evolved gases were analyzed with a quadrupole mass spectrometer Omnistar mod GSD 320. The masses of H_2S, SO_2, CS_2, SO_3 and SO were followed, as sulfur can be desorbed as several species. Moreover the masses of H_2O, CO, CO_2 and O_2, due to oxygen-containing groups, were also followed.

The possible changes of the textural characteristics of graphene resulting from the plasma treatments have been analyzed by Raman spectroscopy and nitrogen adsorption. The Raman spectra were obtained by using a spectrometer (Renishaw, DM LM model) equipped with an adapted confocal microscope (LEIKA) and a 514 nm Ar-ion laser source. The nitrogen adsorption isotherms were measured in ASAP 2020 equipment at 77 K.

Kinetic measurements and adsorption isotherms of Pd^{2+} ions on the parent graphene and on the samples obtained by plasma treatments were carried out at 298.1 K, by using a previously reported procedure [37,38]. In a typical experiment, 0.005 g of the adsorbent were added to 20 mL of an aqueous solution of $[PdCl_4]^{2-}$, at pH 5. The metal solutions were prepared by dissolving K_2PdCl_4 in 1M KCl to guarantee that all the Pd^{2+} in solution is as $PdCl_4^{2-}$ anion [39]. 0.1 M HCl was used to set up the initial pH value. The adsorbate concentration was $3.5 \cdot 10^{-4}$ M for the kinetic measurements while for the adsorption isotherms it ranged from $2.5 \cdot 10^{-5}$ M to 10^{-3} M. The samples were shaken in a thermostated air-incubator until the equilibrium was reached. Then, the $PdCl_4^{2-}$ concentration was analyzed by means of absorbance measurements at 474 nm, using a Perkin-Elmer Lambda 25 spectrophotometer.

The adsorption isotherms were fit to the linear form of the Langmuir Equation (1), where C_e is the adsorbate equilibrium concentration, X is the adsorbed amount, X_m is the maximum adsorption capacity and K_L is the Langmuir constant.

$$\frac{1}{X} = \frac{1}{K_L X_m C_e} + \frac{1}{X_m} \quad (1)$$

Electrochemical tests were performed in an Autolab workstation (PGSTAT 302 N potentiostat/galvanostat (EcoChimie B.V.) with a rotating disk electrode (RDE) system (Metrohm AG, Switzerland), controlled with NOVA v2.0 software. A working electrode tip (glassy carbon disk diameter = 3 mm, Metrohm), an Ag/AgCl reference electrode (in 3 M KCl solution, Metrohm) and a Pt wire (+99.99%, Goodfellow Corp.) as counter electrode were disposed in a three-electrode cell setup. The potentials measured against the Ag/AgCl electrode were converted to the reversible hydrogen electrode (RHE) by using the Nernst equation:

$$E_{RHE} = E_{Ag/AgCl} + 0.059\ pH + E^{\circ}_{Ag/AgCl} \quad (2)$$

where E_{RHE} stands for converted potential vs. RHE, $E^{\circ}_{Ag/AgCl} = 0.197$ V at 25 °C, and $E_{Ag/AgCl}$, the measured potential vs. Ag/AgCl. KOH aqueous solution (0.1 M, pH = 13.0), was employed as basic electrolyte. The glassy carbon disk of RDE tip was polished with 6, 3 and 1 μm particle size diamond polishing pastes and alumina slurry to achieve a mirror-like polished surface, and then rinsed with ultrapure water. The modification consists in the deposition of catalyst dispersion (10 μL) on the polished GC disk via dropping and drying under air flux. The preparation of the material dispersions were carried out by adding 1.0 mg of sample and 20 μL of Nafion to a 250 μL of 2-propanol/water solvent mixture (V:V: = 1:1). Before the depositions, the mixtures were sonicated for 30 min to obtain a highly homogeneous catalyst ink. The catalytic behavior of the samples towards oxygen evolution (OER) was assessed at RT, in N_2-saturated electrolyte and by acquiring the corresponding linear sweep voltammetry (LSV) polarization curves. The LSV curves were registered at 1600 rpm of rotation speed for the RDE, by sweeping the potential at 5 mV s^{-1} from 1.0 to 1.8 V (vs. RHE).

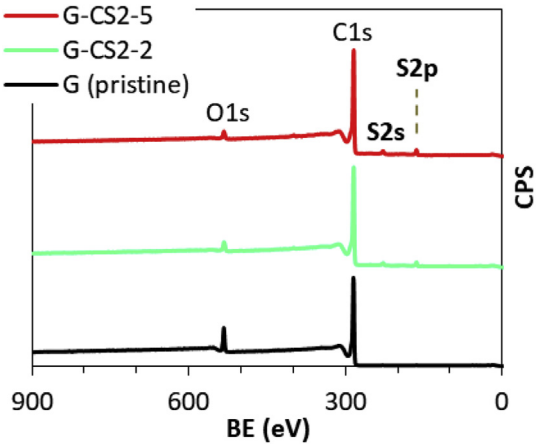

Fig. 2. XPS survey spectra of the pristine graphene and of samples obtained by CS_2 cold plasma treatment for 2 and 5 min. (A colour version of this figure can be viewed online.)

3. Results and discussion

3.1. Sulfur-doped graphene by CS_2 cold plasma

The survey XPS spectra of the original and of two selected plasma treated samples are shown in Fig. 2. The spectrum of the pristine sample present the C 1s and O 1s peaks. Moreover, the spectra of the samples obtained by the CS_2 plasma treatments also show the S 2s and S 2p peaks.

The sulfur contents determined from the XPS spectra range between 1.1 and 2.3 at % (Table 1) in the sample obtained after 5 min of treatment. No larger doping was attained at longer treatments, as already reported for other precursors plasma doping. In spite of this, the value of 2.3 at % is similar to that reported by annealing graphene at 1000 °C with CS_2 and by using graphene oxide which was reduced in a solvothermal process [15]. Moreover our values are slightly larger than those reported when the annealing is carried out between 600 and 1000 °C with an organic sulfur derivative [12,14,15,17]. Thus, if the experimental conditions needed in the reported thermal processes (high temperatures, long heat-treatments, further post-treatments and chemicals) are compared with the CS_2 cold plasma procedure (only the sulfur precursor and 5 min of treatment), it is evident the large advantage of the latter.

The nature of the sulfur containing groups has been analyzed by XPS. Thus, the S 2p high resolution spectrum of a selected sample in Fig. 3, shows the spin-orbit doublet (2p1/2 and 2p3/2, respectively) with a separation of 1.18 eV. The deconvolution of these peaks results in three components, each one of them having the spin-orbit doublet, at 163.7–164.9 eV (of C-S-C/C-S-H groups), 165.0–166.2 eV (of C-SO-C) and 168.0–169.2 eV (of C-SO_2-C) [12,14,15,17]. The

Table 1
Chemical composition of the samples.

	Sample				
	G	G-CS_2-0.5	G-CS_2-1	G-CS_2-2	G-CS_2-5
C (at %)	95.8	95.0	94.5	94.3	94.6
S (at.%)	0.3	1.1	1.1	1.5	2.3
O (at.%)	3.9	3.6	4.4	4.1	3.1

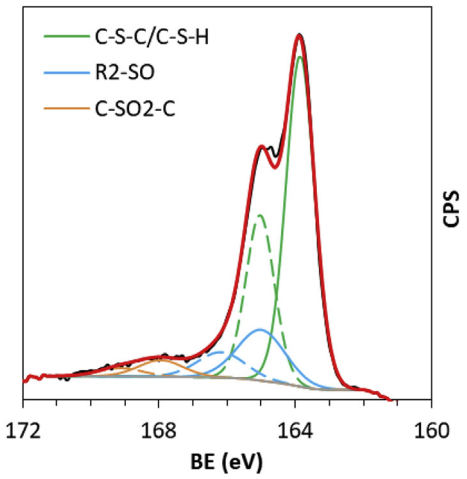

Fig. 3. Deconvolution of the S2p high resolution spectrum of G-CS_2-5. Dashed lines accounts for 1/2 components. (A colour version of this figure can be viewed online.)

Table 2
Results of the deconvolution of the S 2p high resolution XPS spectra.

Sample	S 2p component (%)		
	C-S-C/C-S-H (163.7–164.9 eV)	C-SO-C (165.0–166.2 eV)	C-SO_2-C (168.0–169.2 eV)
G-CS_2-0.5	75.7	17.3	7.0
G-CS_2-1	78.2	14.8	7.0
G-CS_2-2	76.7	13.2	10.1
G-CS_2-5	74.7	19.6	5.7
G-CS_2-5-w	77.6	11.4	11.0

predominant components (around 76%, Table 2) are these assigned to C-S-C or C-S-H of thioether-type or thiol sulfur incorporated into graphene sheets. It is plausible to think that, of these two sulfur-containing groups, the signal is mainly due to C-S-C as the amount of hydrogen in the samples is really very small. Therefore, thioether functions seem to be the prevalent sulfur containing groups fixed by the plasma.

The XPS spectra suggest that sulfur is covalently bonded to graphene. Nevertheless, the thermal stability of the sulfur in the S-doped graphene is a key additional parameter to clarify whether the sulfur is physically adsorbed or it is covalently bonded to the graphene. This was analyzed by TPD. The desorption profiles of CO, CO_2, H_2O and O_2 show (Fig. S1 of Supplementary Information, SI) very small amounts of these molecules, which is probably due to the oxygen is mainly bound to sulfur (Table 2). This statement is supported by the TPD in Fig. 4 which shows the sulfur-containing groups desorb as SO_2, SO (Fig. 4a and b) and CS_2 (Fig. 4c). Desorption profiles from different plasma treated samples have been represented in this figure to show their general TPD characteristics.

The SO_2 profiles (Fig. 4a), which likely account for the C-SO_2-C groups shown in Fig. 3, have a maximum near 260 °C and a band with a relative maximum between 440 and 510 °C. The SO profiles (Fig. 4b), which can be related to the C-SO-C groups, also have a maximum at 260 °C and a band with a maximum between 440 and 510 °C.

In addition the CS_2 profile (Fig. 4c) has a maximum also around 260 °C. This desorption is probably related to sulfur containing groups of type shown in Fig. 5.

The fact that the desorption profiles of SO, SO_2 and CS_2 have a maximum at the same temperature (around 260 °C) suggest that sulfur is forming clusters that decompose at the same temperature rendering these molecules. In addition the profiles are the same in all cases (although the current intensities are different) which

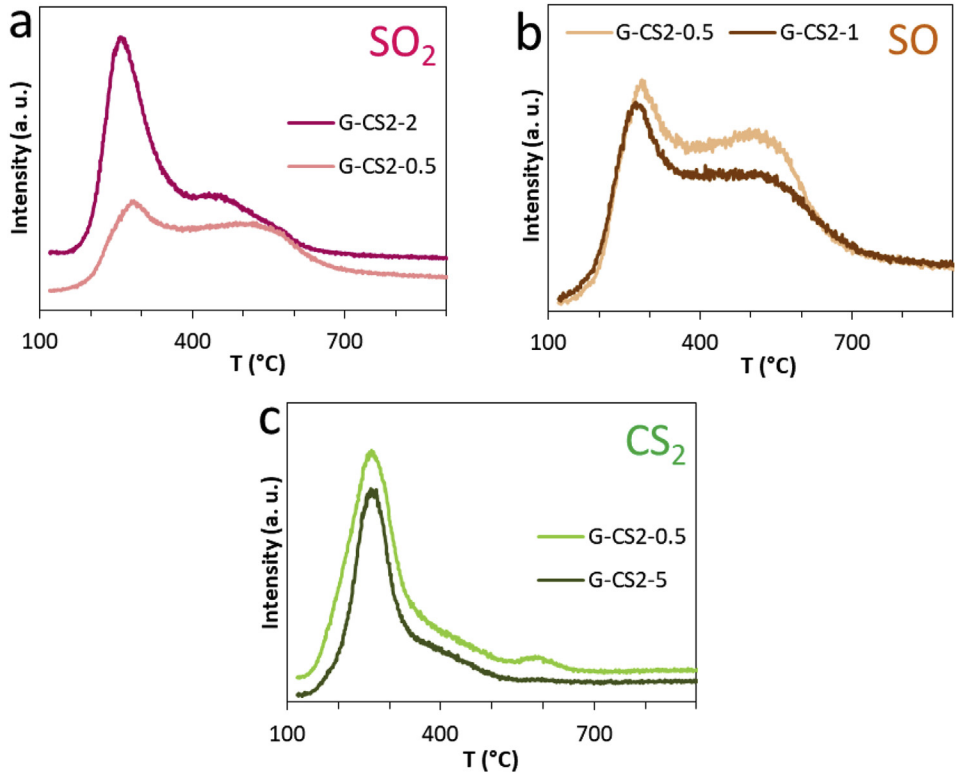

Fig. 4. TPD profiles of SO_2, SO and CS_2 of some selected CS_2-plasma treated samples. (A colour version of this figure can be viewed online.)

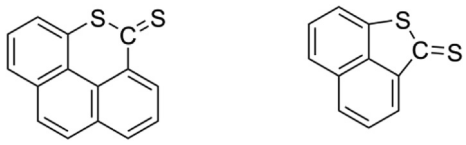

Fig. 5. Representation of -CS_2- groups present in the functionalized samples.

suggests the nature of the sulfur-containing groups is the same regardless the time of treatment. Furthermore, the temperature for the maxima of these profiles are additional evidence that sulfur is covalently bonded to the graphene and support the feasibility of the CS_2 plasma procedure to attach graft sulfur to graphene.

An important aspect is to know the degree of alteration of the graphene sheets as a consequence of the functionalization with sulfur. The analysis of Raman spectra can give insight into this aspect. The Raman spectrum of the pristine graphene is shown in Fig. 6a and these of the samples obtained by treatment with CS_2 plasma are collected in Fig. S2 of SI. The spectra show the most prominent features are the D and G bands (Fig. 6). The former is related to several defects including heteroatoms in the graphene lattice, while the latter is produced by in-plane vibration of sp^2 carbon atoms. The relative large intensity of the D band suggests the pristine material has significant amount of irregularities and defects. The intensity ratio of the D and G bands (at 1336 and 1585 cm^{-1}) of the parent graphene is 1.03, while that of the sulfur-doped sample ranges between 1.05 and 1.01 (Fig. S2 in SI). This suggests the structure of the graphene sheets is scarcely modified as a consequence of the sulfur attachment by the plasma treatment. This behavior is similar to what we have already reported about the functionalization of carbon materials with oxygen and bromine by using the same procedure [5,10]. This is remarkable because in most cases the covalent attachment of heteroatoms to graphene usually results in the formation of defects, leading to the deterioration of the outstanding properties of graphene.

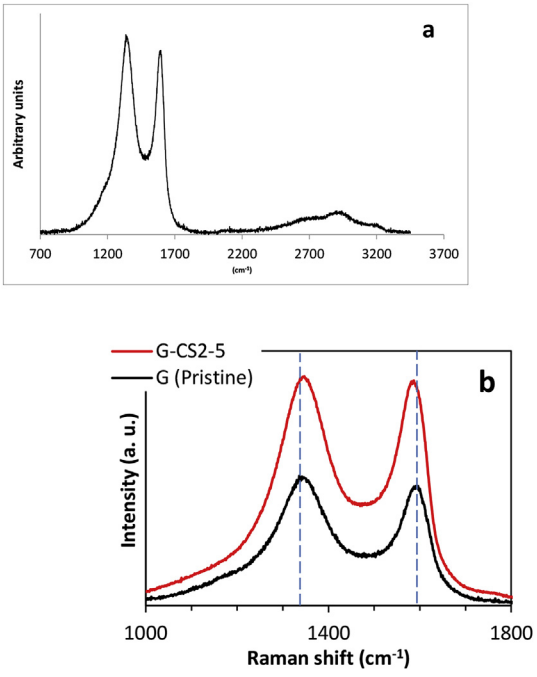

Fig. 6. a) Raman spectrum of the pristine graphene, b) detailed Raman spectra showing the shift of the D and G band due to the covalent attachment of sulfur. (A colour version of this figure can be viewed online.)

In addition the Raman spectra in Fig. 6b provide additional evidence of the sulfur covalent modification of the graphene. Thus, it is seen that after functionalization with sulfur there is an upshift of the D band to 1342 cm^{-1} and a downshift of the G band to 1579 cm^{-1} which are related to n-type doping effect of heteroatoms, sulfur in this case [15,17,40,41]. Therefore, the Raman spectra show the shift of the D and G band due to the covalent attachment of sulfur.

The modification of the textural characteristics of the graphene due to the plasma treatment has been studied by nitrogen adsorption. The surface areas obtained from the isotherms are 468 and 430 $m^2 g^{-1}$, for the parent graphene and for the sample G-CS_2-5, respectively. These values are additional proof of the scarce modification of the graphene texture.

3.2. S/Pd nanoparticles supported on the graphene surface

As commented in the introduction section, the aim behind the preparation of sulfur-doped graphene is not only to test their electrochemical behavior but also to use this material to capture Pd^{2+} from aqueous solutions. For this reason it is very important to know the stability of the sulfur-containing groups in solution. Thus, we have prepared a water suspension of G-CS_2-5 and kept it stirring for 24 h at room temperature. After that, the resulting product, labelled as G-CS_2-5-w (where "w" stands for water), was analyzed by XPS and TPD. A decrease of sulfur content (Table 1), from 2.3 to 1.7 at %, is obtained from XPS spectra but still this sulfur content after the treatment with water is relevant. Moreover there is an increase in oxygen content from 3.1 at % to 6.7 at % (Table 1), which is probably due in part to the hydrolysis of some functional groups as shown in Fig. 7. Dithiocarboxylates are more reactive than carboxylate esters [42]. One of the reasons for its higher reactivity is the poor overlap of 3p orbitals of sulfur with 2p orbitals of carbon to give C=S double bond (what makes the double C=S bond more prone to nucleophilic attack than C=O bonds). Then, the C=S bonds tend to react to transform into C-S single bonds. The scheme of transformation upon reaction with water in Fig. 7 is not other than the final stage of a series of intermediates resulting from nucleophilic attack of water to the carbon atom of C=S and the subsequent displacement of a thiol, or hydrogen sulfide. A detail scheme of the process is shown in Fig. S3 of SI.

Thus, the much larger evolution of hydrogen sulfide in TPD after contact with water has to be related to its reaction with some of the fixed sulfur groups. Thus, it seems reasonable to consider that these groups can receive nucleophilic attack of water to give "addition" intermediates (possessing C-S-H groups, see Fig. S3 of SI). These groups can transform in part into thiocarboxylate groups (with evolution of H_2S, Fig. 7) during the water treatment, or remain as such intermediates, which will release H_2S upon heating during the TPD analysis.

The results for the deconvolution of the sulfur high resolution XPS spectrum for the water-treated sample (bottom line in Table 2) show an increase of the C-SO_2-C groups, while the percentage of C-S-C/C-S-H groups remains almost unchanged. The former also accounts for the increase of the oxygen content already commented. The latter means that the large majority of sulfur is stable towards hydrolysis. Moreover, the fact that the amount C-S-C/C-S-H groups does not change is in agreement with the SO_2 and CS_2 TPD profiles

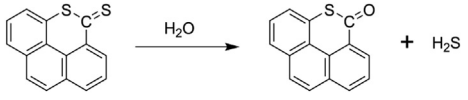

Fig. 7. Hydrolysis of -CS_2- groups (a detail scheme is shown in Fig. S3 of SI).

(Fig. S4 of SI) are similar to these of the parent sample.

Nevertheless, the sample after being in water for 24 h present a desorption profile of SH_2 with a maximum near 315 °C (Fig. 8), which is probably related to some sulfur containing groups have been transformed by hydrolysis into C-S-H. The desorption of SH_2 is almost negligible in the parent sample. The general outcome of these data is that the plasma-synthetized S-doped graphenes can be considered stable in aqueous solution.

Therefore we have selected sample G-CS_2-5 to capture Pd^{2+} from aqueous solution (c.f. experimental section) and the results are compared with these of the parent G sample in Fig. 9. The plots of the kinetics of Pd^{2+} capture in Fig. 9a show the equilibrium is reached in about 10 h in the case of the pristine graphene, and in 40 h in the case of G-CS_2-5. Consequently, 48 h was considered time enough to attain equilibrium at each concentration during the recording of the isotherm. From Fig. 9a and b it is clear that the sample which has covalently-bonded sulfur captures larger amounts of Pd^{2+} than the pristine graphene. Fitting the experimental data of the isotherms to the Langmuir model (equation (1)) allows determining the amounts of Pd^{2+} captured by both samples: 0.19 and 0.72 mmol g^{-1} for the pristine G and G-CS_2-5, respectively. This supports the functionalization of graphene with sulfur by the plasma treatment is an adequate strategy to increase the affinity of graphene towards Pd^{2+} and to achieve significant retention values.

The sample with the highest retention capacity and the original graphene, G, were analyzed by XPS after the isotherm Pd^{2+} experiments. The survey spectra of both samples show the Pd 3d peak and the quantification rendered amounts of Pd of 0.1 and 0.6 mmol g^{-1} for the samples G and G-CS_2-5, respectively, in agreement with the values obtained from the isotherms. In addition, there is an increase in oxygen content up to near 9 at.% and a decrease of sulfur to near 1.3 at % in sample G-CS_2-5, in agreement with the previous result of the stability in aqueous solution of the graphene functionalized with sulfur. Moreover, the spectrum of G after adsorption of Pd^{2+} shows chlorine content of 0.14 at %. This means that the Pd^{2+} is adsorbed, at least in part, as $PdCl_4^{2-}$, i.e. the chemical product used for the adsorption experiments (cf experimental section). Nevertheless, the amount of chlorine is negligible in sample G-CS_2-5 after the retention of Pd^{2+} which points out to a different procedure of capturing the metal ion. The S 2p high resolution spectrum of the sample G-CS_2-5 after the capture of Pd^{2+} (Fig. 10a) shows, just like that of the parent sample (Fig. 3), the components assigned to the C-S-C/C-S-H, C-SO-C and C-SO_2-C groups.

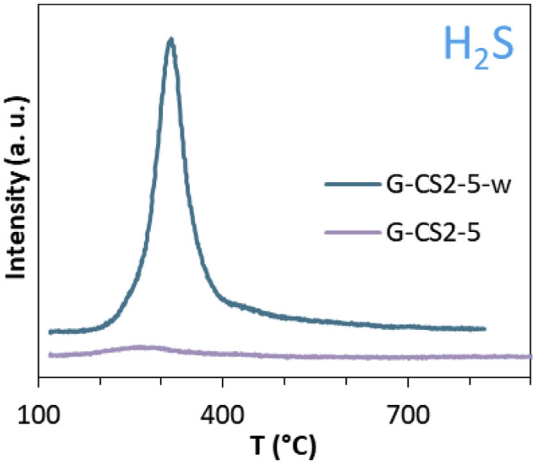

Fig. 8. TPD profile of H_2S of the sample G-CS_2-5 and G-CS_2-5-w. (A colour version of this figure can be viewed online.)

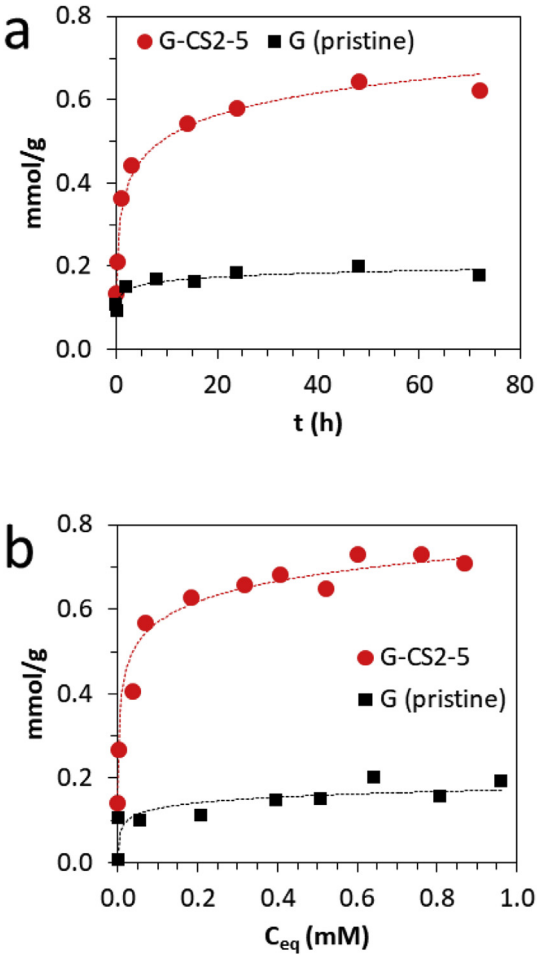

Fig. 9. Capture of Pd^{2+} by G and G-CS_2-5: a) kinetics and b) isotherms. (A colour version of this figure can be viewed online.)

Interestingly a new sulfur component, which is not in the spectrum of sample G-CS_2-5 (Fig. 3), appears at lower binding energies (162.74 and 163.92 eV) after the capture of Pd^{2+}. This new component is associated with metal/sulfur interaction [43–45]. Moreover, the high resolution Pd 3d spectrum (Fig. 10b) shows the two peaks 3/2 and 5/2 at 337.1 and 342.3 eV due to the metal in 2 + oxidation state. Therefore, it is likely the capture of Pd^{2+} by G-CS_2-5 is produced by the covalent interaction with sulfur of thioether or thiolate groups. It is known that in the hard-soft acid-base theory of Pearson, sulfur is a soft base and Pd^{2+} is a soft acid so that the sulfur-Pd^{2+} covalent bond is favored. A consequence of the capture of Pd^{2+} is the new hybrid shows an electronic behavior very different to that of the pristine graphene. The valence band spectrum of the sample with Pd^{2+} (Fig. 10c) has a defined maximum at 3.5 eV, whereas the pristine graphene only shows a band, also present in G-CS_2-5-Pd, with a maximum near 19 eV.

Fig. 11a presents a HRTEM image of the pristine graphene which shows several wrinkles and no evidence of other features on the surface. Nevertheless the two selected HRTEM images of sample G-CS_2-Pd (Fig. 11b and c) show the existence of nanoparticles on the surface of graphene after the capture of Pd^{2+}. The HAADF micrographs obtained by high resolution electron microscopy in STEM mode (Fig. 12) also evidence the presence of the mentioned nanoparticles. The EDX spectrum (Fig. S5 of SI) presents the peaks of sulfur and palladium. Furthermore the maps in Fig. 12 show that both sulfur and palladium are homogeneously distributed on the

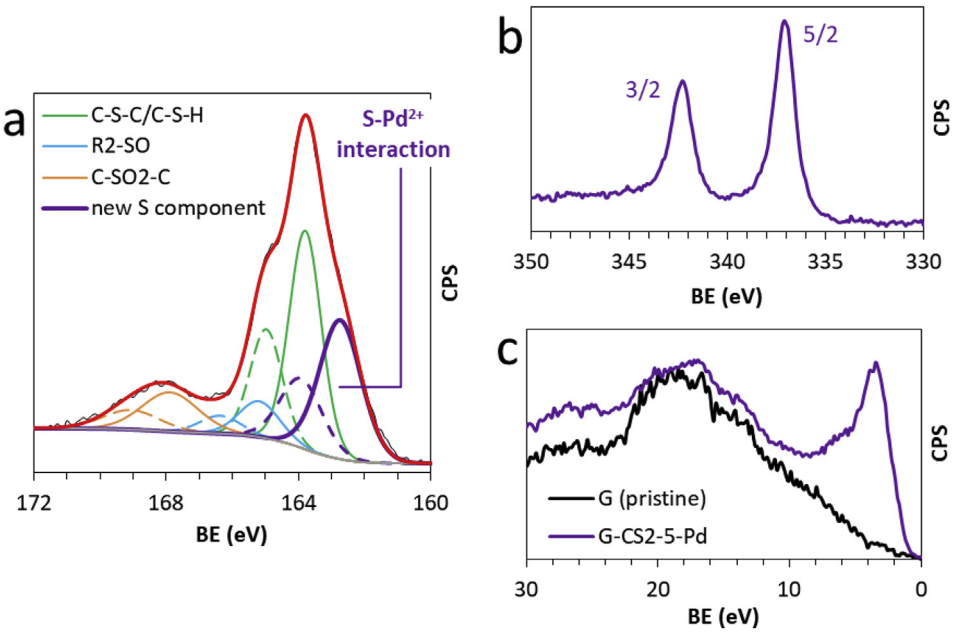

Fig. 10. a) Deconvolution of the S 2p, b) Pd 3d XPS high resolution spectra of G-CS_2-5 after the capture of Pd^{2+} and c) valence band spectra of the pristine graphene and of sample G-CS_2-5-Pd. (A colour version of this figure can be viewed online.)

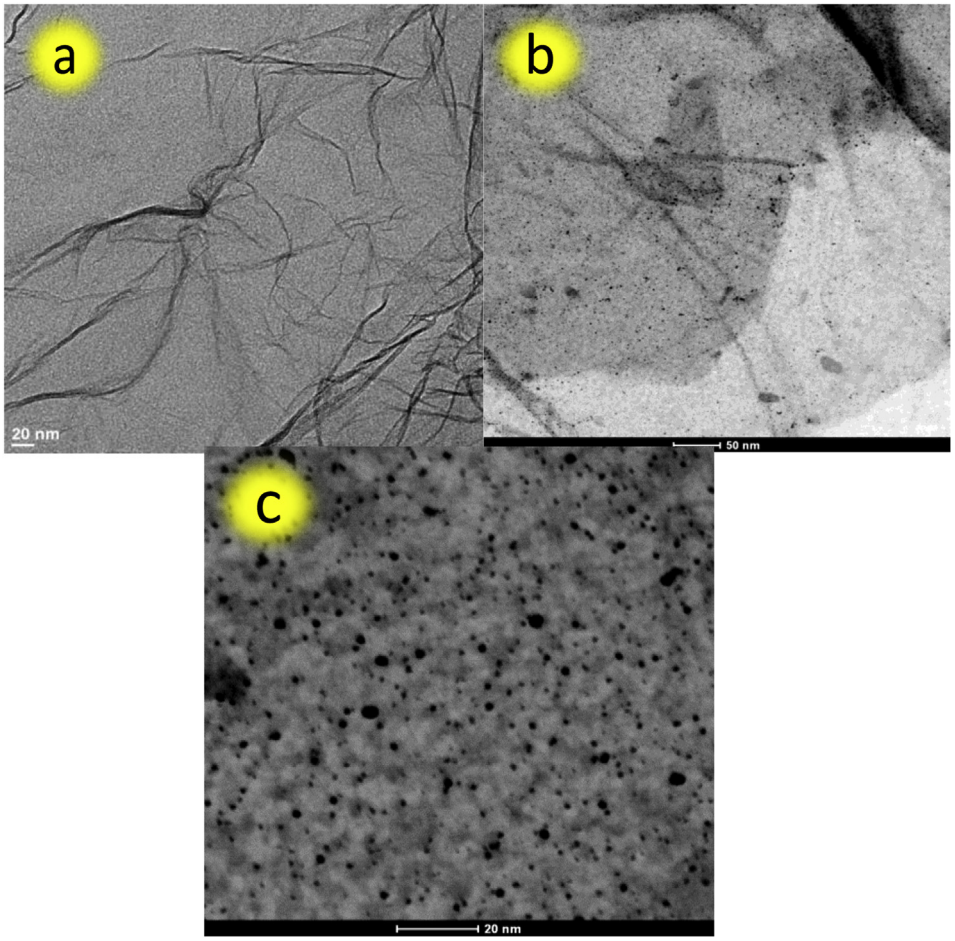

Fig. 11. HRTEM images of a) pristine graphene; b) and c) G-CS_2-Pd at two different magnifications. (A colour version of this figure can be viewed online.)

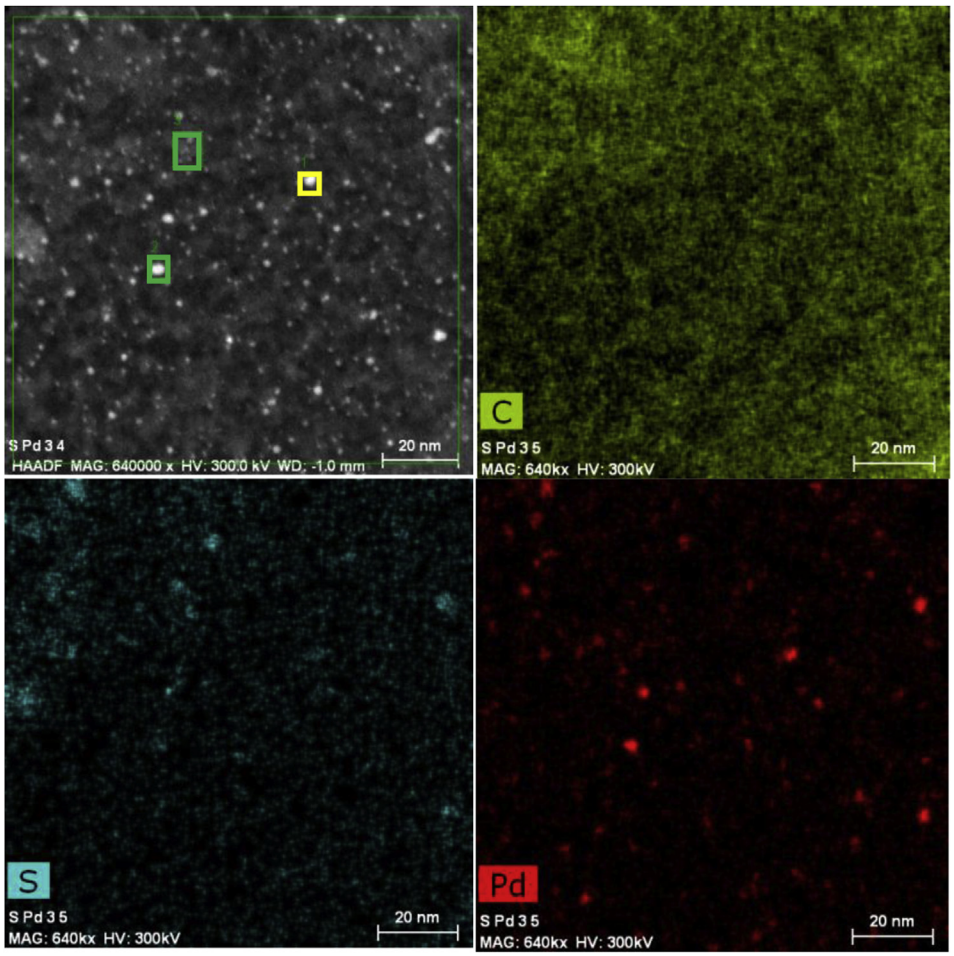

Fig. 12. STEM (HAADF) image with the spots used for EDX (small green and yellow squares) and maps of C, S and Pd. (A colour version of this figure can be viewed online.)

surface of graphene. The statistical analysis of the size of the nanoparticles was carried out by means of ImageJ software [46]. For this purpose we analyzed more than 4600 nanoparticles and Fig. 13 shows the result of the size distribution. The size of most nanoparticles is 2 nm (35%) but there is a significant amount (27%) of 3 nm, so that the vast majority of them appear in a narrow distribution in the range 2–3 nm. All these data suggest the nanoparticles on the surface of graphene are sulfur(thioether/thiolate)-palladium clusters. Moreover, these data also show up the sulfur doping of graphene is able to control the nucleation of the sulfur(thioether/thiolate)-palladium clusters rendering a homogenous size-distribution of nanoparticles.

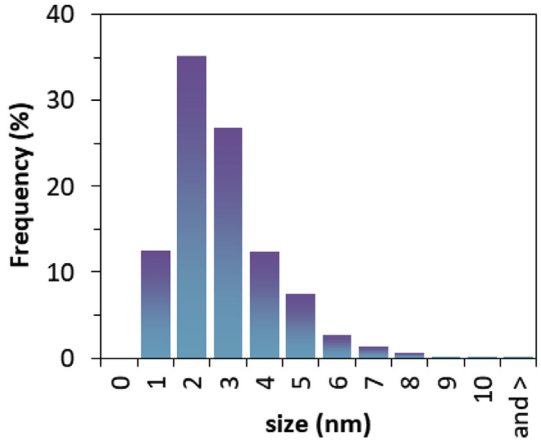

Fig. 13. Sulfur-Pd nanoparticle size distribution on the surface of graphene. (A colour version of this figure can be viewed online.)

3.3. Electrocatalytic behavior

We have studied the catalysis of the OER in order to assess the effect of sulfur and S-Pd doping on the graphene catalytic activity. For that, the LSV plots for the pristine graphene, two derived plasma-treated samples (G-CS_2-2 and G-CS_2-5) and G-CS_2-5-Pd were obtained (Fig. 14).

The polarization curve of the sample G-CS_2-2 shows an almost unchanged current density in relation to that of the pristine graphene. The sample G-CS_2-5 exhibits a very drastic increase of catalytic activity. Thus, the increase of S-containing functions up to 1.5 at % in G-CS_2-2 results in a negligible rise of current density (Fig. 14b). Nevertheless, when the amount of functions rises up to 2.3 at % in G-CS_2-5, the catalytic activity is boosted, producing a significant current density increase of a ≈325% with respect to that achieved by the pristine graphene (Fig. 14b). This non-linear relationship of the current density in OER tests can be related to the concentration and nature of the sulfur-containing groups. Nevertheless, it is necessary to remember that the nature of the sulfur-containing groups of all the samples is similar regardless the time of treatment (see above comments about the TPD profiles in Fig. 4).

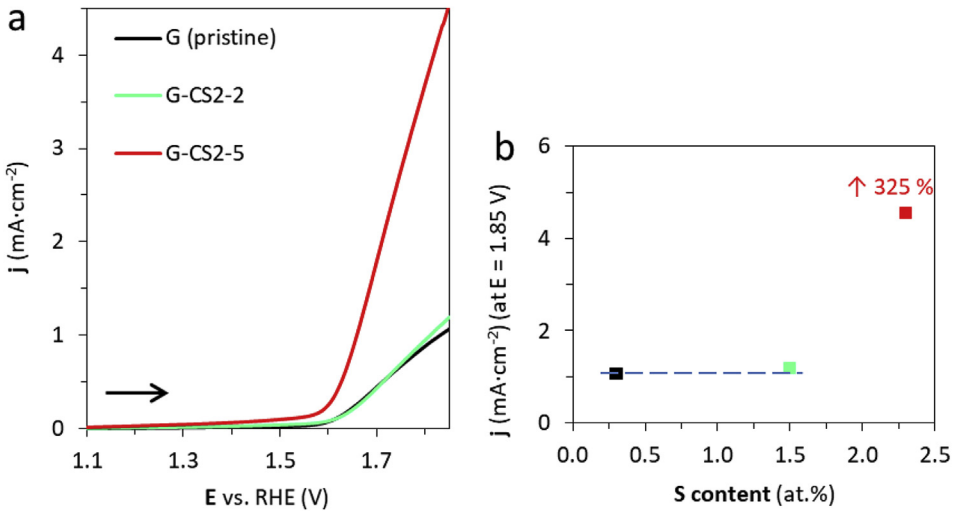

Fig. 14. a) LSV curves for G, G-CS_2-2 and G-CS_2-5 (KOH 0.1 M solution, scan rate = 5 mV s^{-1}, rotation speed = 1600 rpm), and b) variation of the maximum current density with the S atomic concentration. (A colour version of this figure can be viewed online.)

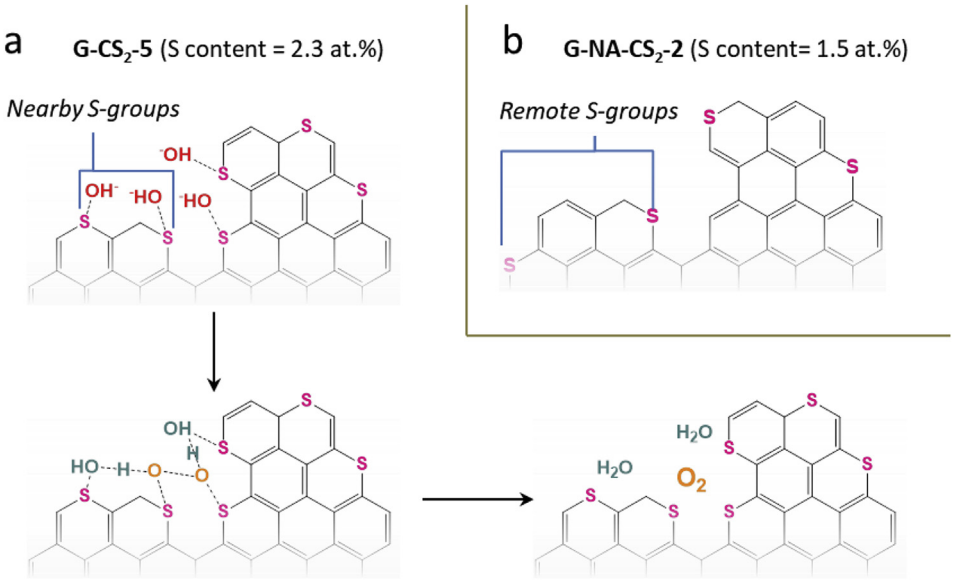

Fig. 15. a) Proposed mechanism for the OER process catalyzed by sample G-CS_2-5, and b) scheme of S-group distribution in G-CS_2-2. (A colour version of this figure can be viewed online.)

Therefore, this suggests that not only the concentration of the S atoms but also the specific distribution (in terms of proximity) of the sulfur moieties has influence on the catalytic properties. Due to the close confinement of the grafted S groups to the most reactive regions within graphene layers, such as edges and defect clusters, (pointed out by the preservation of I_D/I_G ratios in Raman spectra, c.f. Fig. 6), the 0.8 at % increase in sulfur content from G-CS_2-2 to G-CS_2-5 probably results in a significant decrease in the average distance between adjacent S atoms in G-CS_2-5 (Fig. 15b).

This change in the sulfur atoms distribution likely leads to a closer proximity of the hydroxyl groups (initial reagents of OER in alkaline media), promoting the reaction between them to produce O_2 and H_2O during the catalyzed process (Fig. 15a). Therefore, the concentration degree of S moieties within graphene edges and defects (limited regions in comparison with the whole graphene layers) seems to be a more determining factor than the overall S concentration and the proportion of the different types of S-groups [17], since both factors are relatively similar for G-CS_2-2 and G-CS_2-5.

4. Conclusions

The successful application of CS_2 cold plasmas to the preparation of S-doped graphene has been reported for the first time. The generation of very reactive sulfur species from CS_2 vapor allows obtaining S-doped graphenes in a very simple procedure, avoiding conventional energy/time-consuming treatments. Remarkably, CS_2 plasma treatment of only 5 min produces doped samples containing 2.3 at % of sulfur which is covalently bond to graphene. Sulfur is attached forming different functions, been thioether prevalent. These sulfur containing groups show good thermal stability and most of them are also stable in aqueous medium. In addition, the integration of the S-atoms into the graphene layers does not

generate significant defects, preserving the original structural order of pristine graphene.

The fast and simple S-doping of graphene described in this work also has a direct impact on graphene properties. Thus, the functionalization with sulfur notably improves the Pd^{2+} retention capacity of graphene: from 0.19 (in the case of pristine graphene) to 0.72 mmol g^{-1} (in the case of the graphene exhibiting the highest doping degree, G-CS_2-5). This allows the formation of sulfur-Pd nanoclusters supported on the surface of graphene. Moreover, the electrocatalytic activity towards OER of G-CS_2-5 is drastically increased, quadrupling the current density achieved by the undoped material. These results clearly show up the outstanding potential of CS_2 plasmas regarding the efficient doping of graphene materials and the enhancement of their interesting features.

Acknowledgements

The financial support of the MINECO (projects MAT2014-60104-C2-1-R and MAT2014-60104-C2-2-R), FEDER program, Autonomous Regional Government (J. de Andalucía, grupo RNM342) and Programa de Fortalecimiento de la I+D+i from UGR is acknowledged. The technical assistance of Centre of Instrumental Facilities, STI, of the University of Jaén is also acknowledged. The work was also funded by Fundação para a Ciência e a Tecnologia de Portugal (FCT)/MEC under FEDER under Program PT2020 - project UID/QUI/50006/2013-POCI/01/0145/FEDER/007265 and project "UniRCell", with the reference POCI-01-0145-FEDER-016422. Víctor K. Abdelkader Fernández thanks UniRCell project for the post-doctoral grant.

Appendix A. Supplementary data

Supplementary data to this article can be found online at https://doi.org/10.1016/j.carbon.2018.12.045.

References

[1] J. Sturala, J. Luxa, M. Pumera, Z. Sofer, Chemistry of graphene derivatives: synthesis, applications, and perspectives, Chem. Eur. J. 24 (2018) 5992–6006, https://doi.org/10.1002/chem.201704192.
[2] C. Hu, D. Liu, Y. Xiao, L. Dai, Functionalization of graphene materials by heteroatom-doping for energy conversion and storage, Prog. Nat. Sci. Mater. Int. 28 (2018) 121–132, https://doi.org/10.1016/j.pnsc.2018.02.001.
[3] X. Xu, C. Liu, Z. Sun, T. Cao, Z. Zhang, E. Wang, Z. Liu, K. Liu, Interfacial engineering in graphene bandgap, Chem. Soc. Rev. 47 (2018) 3029–3099, https://doi.org/10.1039/c7cs00836h.
[4] U.N. Maiti, W.J. Lee, J.M. Lee, Y. Oh, J.Y. Kim, J.E. Kim, J. Shim, T.H. Han, S.O. Kim, 25th anniversary article: chemically modified/doped carbon nanotubes & graphene for optimized nanostructures & nanodevices, Adv. Mater. 26 (2014) 40–67, https://doi.org/10.1002/adma.201303265.
[5] F. Morales-Lara, M.J. Pérez-Mendoza, D. Altmajer-Vaz, M. García-Román, M. Melguizo, F.J. López-Garzón, M. Domingo-García, Functionalization of multiwall carbon nanotubes by ozone at basic pH. Comparison with oxygen plasma and ozone in gas phase, J. Phys. Chem. C. 117 (2013) 11647–11655, https://doi.org/10.1021/jp4017097.
[6] V.K. Abdelkader, S. Scelfo, C. García-Gallarín, M.L. Godino-Salido, M. Domingo-García, F.J. López-Garzón, M. Pérez-Mendoza, Carbon tetrachloride cold plasma for extensive chlorination of carbon nanotubes, J. Phys. Chem. C. 117 (2013) 16677–16685, https://doi.org/10.1021/jp404390h.
[7] V.K. Abdelkader, M. Domingo-García, M.D. Gutiérrez-Valero, R. López-Garzón, M. Melguizo, C. García-Gallarín, F.J. Lopez-Garzon, M.J. Pérez-Mendoza, Sidewall chlorination of carbon nanotubes by iodine trichloride, J. Phys. Chem. C. 118 (2014) 2641–2649, https://doi.org/10.1021/jp411935g.
[8] V.K. Abdelkader-Fernández, F. Morales-Lara, M. Melguizo, C. García-Gallarín, R. López-Garzón, M.L. Godino-Salido, F.J. López-Garzón, M. Domingo-García, M.J. Pérez-Mendoza, Degree of functionalization and stability of fluorine groups fixed to carbon nanotubes and graphite nanoplates by CF4 microwave plasma, Appl. Surf. Sci. 357 (2015) 1410–1418, https://doi.org/10.1016/j.apsusc.2015.09.262.
[9] J.P. Paraknowitsch, A. Thomas, Doping carbons beyond nitrogen: an overview of advanced heteroatom doped carbons with boron, sulphur and phosphorus for energy applications, Energy Environ. Sci. 6 (2013) 2839, https://doi.org/10.1039/c3ee41444b.
[10] V.K. Abdelkader, M. Domingo-García, M. Melguizo, R. López-Garzón, F. Javier López-Garzón, M. Pérez-Mendoza, Covalent bromination of multi-walled carbon nanotubes by iodine bromide and cold plasma treatments, Carbon 93 (2015) 276–285, https://doi.org/10.1016/j.carbon.2015.05.070.
[11] M. Seredych, E. Rodriguez-Castellon, T.J. Bandosz, Alterations of S-doped porous carbon-rGO composites surface features upon CO2 adsorption at ambient conditions, Carbon 107 (2016) 501–509, https://doi.org/10.1016/j.carbon.2016.06.028.
[12] L. Chen, X. Cui, Y. Wang, M. Wang, R. Qiu, Z. Shu, L. Zhang, Z. Hua, F. Cui, C. Weia, J. Shi, One-step synthesis of sulfur doped graphene foam for oxygen reduction reactions, Dalt. Trans. 43 (2014) 3420–3423, https://doi.org/10.1039/c3dt52253a.
[13] W. Kicinski, M. Szala, M. Bystrzejewski, Sulfur-doped porous carbons: synthesis and applications, Carbon 68 (2014) 1–32, https://doi.org/10.1016/j.carbon.2013.11.004.
[14] D. Higgins, M.A. Hoque, M.H. Seo, R. Wang, F. Hassan, J.-Y. Choi, M. Pritzker, A. Yu, J. Zhang, Z. Chen, Development and simulation of sulfur-doped graphene supported platinum with exemplary stability and activity towards oxygen reduction, Adv. Funct. Mater. 24 (2014) 4325–4336, https://doi.org/10.1002/adfm.201400161.
[15] J. Park, Y.J. Jang, Y.J. Kim, M. Song, S. Yoon, D.H. Kim, S.-J. Kim, Sulfur-doped graphene as a potential alternative metal-free electrocatalyst and Pt-catalyst supporting material for oxygen reduction reaction, Phys. Chem. Chem. Phys. 16 (2014) 103–109, https://doi.org/10.1039/c3cp54311k.
[16] T.J. Bandosz, M. Seredych, E. Rodriguez-Castellon, Y. Cheng, L.L. Daemen, A.J. Ramirez-Cuesta, Evidence for CO2 reactive adsorption on nanoporous S- and N-doped carbon at ambient conditions, Carbon 96 (2016) 856–863, https://doi.org/10.1016/j.carbon.2015.10.007.
[17] Z. Yang, Z. Yao, G. Li, G. Fang, H. Nie, Z. Liu, X. Zhou, X. Chen, S. Huang, Sulfur-doped graphene as an efficient metal-free cathode catalyst for oxygen reduction, ACS Nano 6 (2012) 205–211, https://doi.org/10.1021/nn203393d.
[18] Y.S. Yun, V.D. Le, H. Kim, S.J. Chang, S.J. Baek, S. Park, B.H. Kim, Y.H. Kim, K. Kang, H.J. Jin, Effects of sulfur doping on graphene-based nanosheets for use as anode materials in lithium-ion batteries, J. Power Sources 262 (2014) 79–85, https://doi.org/10.1016/j.jpowsour.2014.03.084.
[19] J. Han, B. Xi, Z. Feng, X. Ma, J. Zhang, S. Xiong, Y. Qian, Sulfur-hydrazine hydrate-based chemical synthesis of sulfur@graphene composite for lithium-sulfur batteries (vol 5, pg 785, 2018, Inorg. Chem. Front. 5 (2018) 962–963, https://doi.org/10.1039/c8qi90007h.
[20] H.C. Chin, Preparation and characterization of carbon-sulfur surface compounds, Carbon 19 (1981) 175–186, https://doi.org/10.1016/0008-6223(81)90040-3.
[21] C. Moreno-Castilla, I. Fernandez-Morales, M. Domingo-Garcia, F.J. Lopez-Garzon, Carbon molecular sieves produced by the fixation of sulfur surface complexes, Chromatographia 20 (1985) 709–712.
[22] Z.J. Han, A.T. Murdock, D.H. Seo, A. Bendavid, Recent progress in plasma-assisted synthesis and modification of 2D materials, 2D Mater. 5 (2018), 032002, https://doi.org/10.1088/2053-1583/aabb81.
[23] A.J. McCue, A. Guerrero-Ruiz, I. Rodríguez-Ramos, J.A. Anderson, Palladium sulphide – a highly selective catalyst for the gas phase hydrogenation of alkynes to alkenes, J. Catal. 340 (2016) 10–16, https://doi.org/10.1016/j.jcat.2016.05.002.
[24] P. Geng, S. Zheng, H. Tang, R. Zhu, L. Zhang, S. Cao, H. Xue, H. Pang, Transition metal sulfides based on graphene for electrochemical energy storage, Adv. Energy Mater. 8 (2018) 1703259, https://doi.org/10.1002/aenm.201703259.
[25] L. Shen, J. Wang, G. Xu, H. Li, H. Dou, X. Zhang, NiCo2S4 nanosheets grown on nitrogen-doped carbon foams as an advanced electrode for supercapacitors, Adv. Energy Mater. 5 (2015) 1400977, https://doi.org/10.1002/aenm.201400977.
[26] J. Xie, S. Liu, G. Cao, T. Zhu, X. Zhao, Self-assembly of CoS2/graphene nanoarchitecture by a facile one-pot route and its improved electrochemical Li-storage properties, Nano Energy 2 (2013) 49–56, https://doi.org/10.1016/j.nanoen.2012.07.010.
[27] G. Huang, H. Liu, S. Wang, X. Yang, B. Liu, H. Chen, M. Xu, Hierarchical architecture of WS2 nanosheets on graphene frameworks with enhanced electrochemical properties for lithium storage and hydrogen evolution, J. Mater. Chem. A. 3 (2015) 24128–24138, https://doi.org/10.1039/c5ta06840a.
[28] G. Zhao, X. Li, M. Huang, Z. Zhen, Y. Zhong, Q. Chen, X. Zhao, Y. He, R. Hu, T. Yang, R. Zhang, C. Li, J. Kong, J. Bin Xu, R.S. Ruoff, H. Zhu, The physics and chemistry of graphene-on-surfaces, Chem. Soc. Rev. 46 (2017) 4417–4449, https://doi.org/10.1039/c7cs00256d.
[29] H. Cheng, Y. Huang, G. Shi, L. Jiang, L. Qu, Graphene-based functional architectures: sheets regulation and macrostructure construction toward actuators and power generators, Acc. Chem. Res. 50 (2017) 1663–1671, https://doi.org/10.1021/acs.accounts.7b00131.
[30] X. Gong, G. Liu, Y. Li, D.Y.W. Yu, W.Y. Teoh, Functionalized-graphene composites: fabrication and applications in sustainable energy and environment, Chem. Mater. 28 (2016) 8082–8118, https://doi.org/10.1021/acs.chemmater.6b01447.
[31] S. Ren, P. Rong, Q. Yu, Preparations, properties and applications of graphene in functional devices: a concise review, Ceram. Int. 44 (2018) 11940–11955, https://doi.org/10.1016/j.ceramint.2018.04.089.
[32] M. Zhang, C. Hou, A. Halder, H. Wang, Q. Chi, Graphene papers: smart architecture and specific functionalization for biomimetics, electrocatalytic sensing

and energy storage, Mater. Chem. Front. 1 (2017) 37–60, https://doi.org/10.1039/c6qm00145a.
[33] T.H. Han, N. Parveen, S.A. Ansari, J.H. Shim, A.T.N. Nguyen, M.H. Cho, Electrochemically synthesized sulfur-doped graphene as a superior metal-free cathodic catalyst for oxygen reduction reaction in microbial fuel cells, RSC Adv. 6 (2016) 103446–103454, https://doi.org/10.1039/c6ra14114e.
[34] Y. Li, C. He, L. Zhang, Identification of the active sites in sulfur-doped graphene for oxygen reduction reaction: the keyrole of dissociated O2 adsorption, Solid State Commun. 267 (2017) 33–38, https://doi.org/10.1016/j.ssc.2017.09.005.
[35] S. Oh, J. Kim, M. Kim, D. Nam, J. Park, E. Cho, H. Kwon, Synergetic effects of edge formation and sulfur doping on the catalytic activity of a graphene-based catalyst for the oxygen reduction reaction, J. Mater. Chem. A. 4 (2016) 14400–14407, https://doi.org/10.1039/c6ta05020d.
[36] C. Zhai, M. Sun, M. Zhu, S. Song, S. Jiang, A new method to synthesize sulfur-doped graphene as effective metal-free electrocatalyst for oxygen reduction reaction, Appl. Surf. Sci. 407 (2017) 503–508, https://doi.org/10.1016/j.apsusc.2017.02.191.
[37] M. Luz Godino-Salido, A. Santiago-Medina, P. Arranz-Mascaros, R. Lopez-Garzon, M.D. Gutierrez-Valero, M. Melguizo, F. Javier Lopez-Garzon, Novel active carbon/crown ether derivative hybrid material for the selective removal of Cu(II) ions: the crucial role of the surface chemical functions, Chem. Eng. Sci. 114 (2014) 94–104, https://doi.org/10.1016/j.ces.2014.04.014.
[38] M. Luz Godino-Salido, R. Lopez-Garzon, M.D. Gutierrez-Valero, P. Arranz-Mascaros, M. Melguizo-Guijarro, M.D. de la Torre, V. Gomez-Serrano, M. Alexandre-Franco, D. Lozano-Castello, D. Cazorla-Amoros, M. Domingo-Garcia, Effect of the surface chemical groups of activated carbons on their surface adsorptivity to aromatic adsorbates based on pi-pi interactions, Mater. Chem. Phys. 143 (2014) 1489–1499, https://doi.org/10.1016/j.matchemphys.2013.12.005.
[39] C.F. Baes, R.E. Mesmer, The Hydrolysis of Cations, John Wiley & Sons Inc, New York, USA, 1976.
[40] F. Shahzad, P. Kumar, Y.H. Kim, S.M. Hong, C.M. Koo, Biomass-derived thermally annealed interconnected sulfur-doped graphene as a shield against electromagnetic interference, ACS Appl. Mater. Interfaces 8 (2016) 9361–9369, https://doi.org/10.1021/acsami.6b00418.
[41] G. Ning, X. Ma, X. Zhu, Y. Cao, Y. Sun, C. Qi, Z. Fan, Y. Li, X. Zhang, X. Lan, J. Gao, Enhancing the Li storage capacity and initial coulombic efficiency for porous carbons by sulfur doping, ACS Appl. Mater. Interfaces 6 (2014) 15950–15958, https://doi.org/10.1021/am503716k.
[42] J. Grote, F. Friedrich, K. Berthold, L. Hericks, B. Neumann, H.-G. Stammler, N.W. Mitzel, Dithiocarboxylic acids: an old theme revisited and augmented by new preparative, spectroscopic and structural facts, Chem. Eur. J. 24 (2018) 2626–2633, https://doi.org/10.1002/chem.201704235.
[43] P. Gobbo, M.C. Biesinger, M.S. Workentin, Facile synthesis of gold nanoparticle (AuNP)-carbon nanotube (CNT) hybrids through an interfacial Michael addition reaction, Chem. Commun. 49 (2013) 2831–2833, https://doi.org/10.1039/c3cc00050h.
[44] P. Gobbo, S. Novoa, M.C. Biesinger, M.S. Workentin, Interfacial strain-promoted alkyne-azide cycloaddition (I-SPAAC) for the synthesis of nanomaterial hybrids, Chem. Commun. 49 (2013) 3982–3984, https://doi.org/10.1039/c3cc41634h.
[45] P. Gobbo, Z. Mossman, A. Nazemi, A. Niaux, M.C. Biesinger, E.R. Gillies, M.S. Workentin, Versatile strained alkyne modified water-soluble AuNPs for interfacial strain promoted azide-alkyne cycloaddition (I-SPAAC), J. Mater. Chem. B. 2 (2014) 1764–1769, https://doi.org/10.1039/c3tb21799j.
[46] W. Rasband, Image J. (2015). https://imagej.nih.gov/ij/.